Effects of Shear Stress in Teletaction and Human Perception

by Gabriel Moy

Research Project

Submitted to the Department of Electrical Engineering and Computer Sciences, University of California at Berkeley, in partial satisfaction of the requirements for the degree of **Master of Science, Plan II**.

Approval for the Report and Comprehensive Examination:

Committee:

Ron Fearing
Research Advisor

Date

* * * * * *

Frank Tendick
Second Reader

Date

Contents

Acknowledgments

I would like to thank Professor Ron Fearing for his guidance, encouragement, and support, and Professor Frank Tendick for his suggestions and comments on the final draft. I would also like to thank Ken Chiang, Joseph Yan, and Wolfgang Zesch for their suggestions and feedback, and many thanks to my parents for their support and encouragement.

This work was supported by NSF Grant IRI-9531837

Abstract

An ideal tactile stimulator would control both normal and shear stress distributions on a user's skin. Since generating normal and shear stress is more difficult than generating only a normal stress, we set up a series of experiments to measure performance differences in a tactile display with and without shear stress information transmission. Psychophysical experiments measured the effect of shear stress information on the perception of static stimuli. Wax blocks with horizontal or vertical grating orientations were used as stimuli. Elastic layers, representing the anti-aliasing filter on a tactile sensor and the reconstruction filter on the tactile display, were placed over the stimuli. In the first experiment, we used two elastic layers in intimate contact as the filters. In the second experiment, we used two elastic layers with a lubricant in between as the filters. The lubricant reduces the shear stress information from being passed to the second elastic layer. A simple planar linear elastic model predicts better high frequency response with no shear information transmitted at the boundary between elastic layers. We tested 10 subjects to measure if there was a performance difference in detecting the orientation of the stimuli. We found that with the lubricant the subjects did better in discriminating orientations at all frequencies used. From the model and results, we show that a tactile stimulator provides greater sensitivity without shear stress albeit with poorer fidelity.

1 Introduction

Information about texture, local compliance, and local shape is important in applications such as telesurgery or handling of fragile objects in telerobotics. A teletaction system comprised of a tactile sensor, a communications channel, and a tactile display or stimulator can be used to provide such information. Figure 1 shows a general configuration of a teletaction system. One possible application is on a robotic laparoscopic telesurgery system. The tactile sensor is mounted on the end effector (the laparoscopic instrument), and the tactile stimulator display is mounted on the master manipulator (the user interface). Ideally, the patterns felt by the user would be indistinguishable from direct contact with the environment. For this, the tactile stimulator needs to generate surface stresses that realistically represent the stresses on the surface of the tactile sensor. To fully control surface stress, the ideal tactile display system should be an infinitely dense array of 3 DOF actuators, which can produce arbitrary normal and shear stress distributions. This paper examines the perceptual difference between a 1 DOF and 3 DOF tactile display for simple grating patterns.

Tactile displays can produce either displacements or forces. In a displacement display, an array of pins is shaped into a contour. In a force display, the pin array will produce a

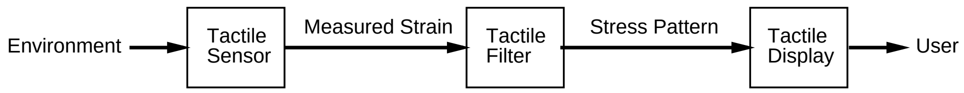

Figure 1: A block diagram representation of a teletaction system.

surface stress distribution representing the data. For a force display, we examine the effects of reducing the amount of shear stress information transmitted. As seen in the Sensopad[1], a device to aid in breast self examinations, reduction of shear stress can enhance detection of embedded objects. There was enhanced detection of surface roughness when a piece of paper, used to reduce shear, was placed between the finger and sandpaper [Lederman 1978].

Most tactile display systems use an array of actuated 1 DOF pins to stimulate the slowly adapting afferent (SA I) units. The density of the stimulator array is limited by actuator size. Currently, the spacing between the centers of the pins is around 2 mm [Cohn et al 1992; Howe et al 1995]. The array is covered by an elastic layer which functions as an anti-aliasing filter. Without the anti-aliasing filter, the user would feel an array of pins instead of a smooth continuous surface. Until actuator technology advances to the point where pin density equals mechanoreceptor density, an anti-aliasing filter will be needed. Even when actuator densities are high enough, an elastic layer will still be needed to protect users from the small display pins stabbing into the skin.

The teletaction problem can be split into three parts, a sensor side, a stimulator (or display) side, and a communications channel (Figure 2) [Fearing et al 1997]. In our case, the communications channel is a direct contact between the sensor and the stimulator to avoid aliasing problems. The sensor is represented by one elastic layer, and the display is represented by another elastic layer. By controlling the boundary conditions between the "sensor" layer and the "stimulator" layer, we can physically simulate 1 DOF and 3 DOF tactile displays. We assume that contact stresses are not affected by this subsurface boundary change. We test human perception of gratings to determine if an array of 1 DOF actuators would be as effective as an array of 3 DOF actuators.

One of the elastic layer combinations consists of two 1 mm thick pieces of silicone rubber (Dow Corning's HSII). Assuming perfect adhesion at the boundary between layers, full normal and shear stress information is transmitted between the tactile sensor and display.

[1]Inventive Products, Inc., Decatur, IL

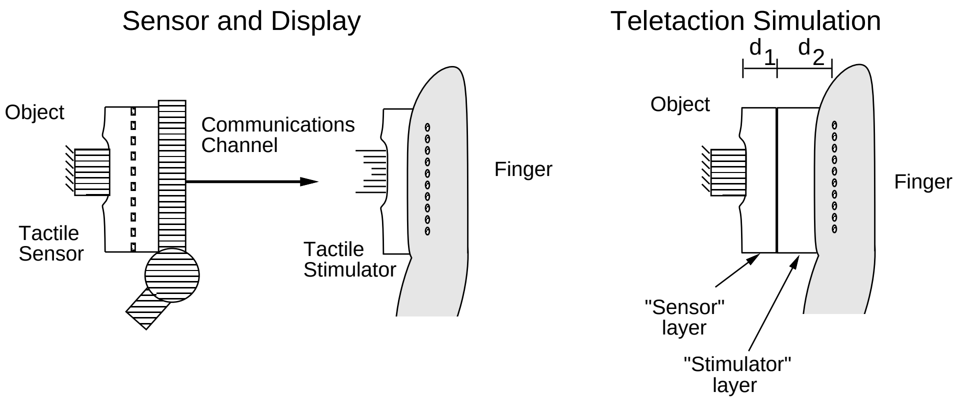

Figure 2: Teletaction with a) a sensor and display, b) elastic layers.

The other elastic layer combination consists of two 1 mm thick pieces of HSII with a thin layer of lubricant between them. Full normal stress information but reduced shear stress information is transmitted between the tactile sensor and display.

1.1 Previous Work

Most teletaction work has focused on tactile sensors and stimulators [Shimoga 1992; Howe et al 1995]. Tactile sensors are comparatively well understood [Boie 1984; Fearing 1990; Howe 1994], although generally designed for shape recognition and manipulation tasks, not teletaction. Typical tactile sensors range in size from 1 mm square with 8×8 elements [Gray and Fearing, 1996] to 16 mm square with 8×8 elements [Howe et al 1995] to a 25 mm diameter cylinder with 3×16 elements [Nicolson and Fearing 1995]. These sensors typically respond only to the normal component of strain.

Tactile display designs have used solenoids [Fischer et al, 1995], shape memory alloys [Howe et al 1995; Hasser and Daniels 1996], pneumatics [Cohn et al 1992], electrostatics [Beebe et al 1995], and tangential tactors using linear microactuators [Ghodssi et al 1996]. The Optacon[2] was developed in 1970 for sensory substitution in blind subjects. It uses vibration of metal rods as the stimulus to the user. Electrocutaneous stimulation [Kaczmarek et al 1991] is mechanically quite simple; however, the perceptual effects are hard to analyze. An ideal stimulator requires $50Ncm^{-2}$ peak pressure, 4 mm stroke, and 25 Hz bandwidth; that is, a power density of $5Wcm^{-2}$, with 1 mm^{-2} actuator density. A stimulator with a 10x1 array of pins with 3 mm stroke, 30 Hz bandwidth, and 2 mm^{-1} pin density has been

[2]Telesensory Systems, Inc., Mountain View, CA

developed [Wellman et al. 1997]. This stimulator approaches the ideal specifications, but is limited to a single row of pins by design.

Human tactile perception is not as well understood as the human vision system. Some areas, such as human tactile sensing sensitivity, sensor density, and spatial and temporal frequency response have been studied [Phillips and Johnson 1981; Loomis and Lederman 1986; Shimojo et al 1997; Tan 1995; Singh 1997].

1.2 Human Mechanoreceptors

In glabrous skin, there are four types of mechanoreceptors responsible for converting the mechanical deformations of the skin to electrical signals sent to the nerves. The mechanoreceptors are named Merkel disks, Meissner's corpuscles, Pacinian corpuscles, and Ruffini endings, or SA I, FA I, FA II, and SA II, respectively. The four mechanoreceptors are compared in Table 1. The SA units are more sensitive to maintained skin indentation, while the FA units are more sensitive to moving stimuli. The SA I and FA I units have small and well defined receptive fields as opposed to the SA II and FA II units, which have large receptive fields.

Some tactile displays are designed to stimulate the mechanoreceptors by providing a display of shape. This shape representation typically excites the SA I units due to their good spatial resolution, sensitivity to maintained skin indentation, and low frequency. It may also excite the FA I units if the tactile display is running at a high frequency (>8 Hz). The fastest tactile displays are running at less than 50 Hz, which encompasses the SA I unit's easily excitable range, and at the middle of the FA I unit's easily excitable range. The SA I units, are predicted to be about 0.7 to 1.0 mm below the skin surface. This depth is based on models and data collected on macaque monkeys [Phillips and Johnson 1981]. The spatial density of the SA units was determined to be approximately 0.7 sensors per mm^3 [Valbo and Johansson 1979].

1.3 Goals

The goal of this project is to measure performance differences in a tactile display with and without shear stress information transmission. We first developed a simple model to predict the effects when shear stress is not transmitted (Section 2). We then conducted a series of

	FA I	FA II	SA I	SA II
Rate of adaptation	fast	fast	slow	slow
Mean Receptive Area	13 mm^2	101 mm^2	11 mm^2	59 mm^2
Spatial Resolution	poor	very poor	good	fair
Sensory Units	43%	13%	25%	19%
Frequency range for most easily excited	8-64 Hz	>64 Hz	2-32 Hz	< 8 Hz

Table 1: Comparison of the four cutaneous mechanoreceptors (adapted from [Shimoga 1992] and [Johansson et al 1982]).

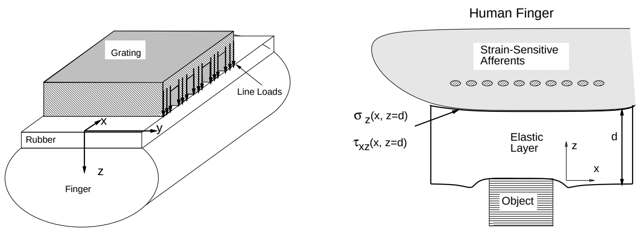

Figure 3: a) Finger and stimuli geometry for plane stress assumption b) slice of the x-z plane.

experiments to measure performance differences in a very simple model teletaction system (Section 3).

2 Model of the Teletaction System

In this section, we describe a model of the interactions between the human finger and normally indented stimuli. We first present the geometry and mechanics of the system. We then model the system using transfer functions.

2.1 Elastic Half Plane Analysis

For a basic model of the sensor, stimulator, and finger, we use the half-plane elastic analysis of [Phillips and Johnson 1981] as a starting point. The plane stress assumption (Figure 3a) is used for our analysis since it is similar to the response of mechanoreceptors in the fingers of macaque monkeys [Phillips and Johnson 1981]. We also assume that the finger senses subsurface normal strain; higher order and more realistic models of the finger are being developed by others, such as [Srinivasan and Dandekar 1996]. Consider a slice of elastic material in the $x-z$ plane (Figure 3b) with the applied force on top constant in the y direction, and the normal stresses on the face of the slice (σ_y) equal to 0.

The stress distribution presented to the finger by the rigid stimuli is modelled as a superposition of line loads applied to the rubber layer. These line loads are constant along the y-axis, but vary along the x-axis. For planar stress analysis, we take a thin slice from the x-z plane, as shown in Figure 3b.

The stresses in the slice for a line load applied normal to the surface are [Johnson 1985]:

$$\sigma_x = \frac{-2F_z z x^2}{\pi r^4} \ , \quad \sigma_z = \frac{-2F_z z^3}{\pi r^4} \ , \quad \tau_{xz} = \frac{-2F_z z^2 x}{\pi r^4} \ ,$$

where F_z is the force per unit thickness of the slice in Nm^{-1}, and $r^2 = x^2 + z^2$. For a concentrated tangential force F_x at the surface:

$$\sigma_x = \frac{-2F_x x^3}{\pi r^4} \ , \quad \sigma_z = \frac{-2F_x x z^2}{\pi r^4} \ , \quad \tau_{xz} = \frac{-2F_x z x^2}{\pi r^4} \ .$$

Since $\sigma_y = 0$ in the plane-stress approximation, the strains ϵ_x and ϵ_z will be a function of only σ_x and σ_z:

$$\epsilon_z = \frac{1}{E}[\sigma_z - \nu\sigma_x] \ , \quad \epsilon_x = \frac{1}{E}[\sigma_x - \nu\sigma_z],$$

where E is the elastic modulus (Nm^{-2}), and ν is Poisson's ratio (typically $\nu \approx 0.5$ for rubber-like materials).

The normal strain ϵ_z has a component $h_z(x,\ z)$ due to F_z and a component $h_x(x,\ z)$ due to the tangential force component F_x . The impulse response for normal strain (with a unit line load applied at angle α) is defined as:

$$h(x,z) = h_z(x,z)\cos\alpha + h_x(x,z)\sin\alpha$$

The normal strain at depth z due to a line load with normal component P and tangential component Q is:

$$\begin{aligned}
\epsilon_z &= \epsilon_{zp} + \epsilon_{zq} = \frac{1}{E}(\sigma_z - \nu\sigma_x) + \frac{1}{E}(\sigma_z - \nu\sigma_x) \\
&= \frac{-2Pz}{\pi E r^4}(z^2 - \nu x^2) + \frac{-2Qxz}{\pi E r^4}(z - \nu x) \\
&= \frac{-2z}{\pi E r^4}(P(z^2 - \nu x^2) + Q(xz - \nu x^2))
\end{aligned}$$

where $E = 4 \times 10^5$ N/m^2 and $\nu = 0.5$. This is not what the human feels, but is a good first order approximation and easy to calculate.

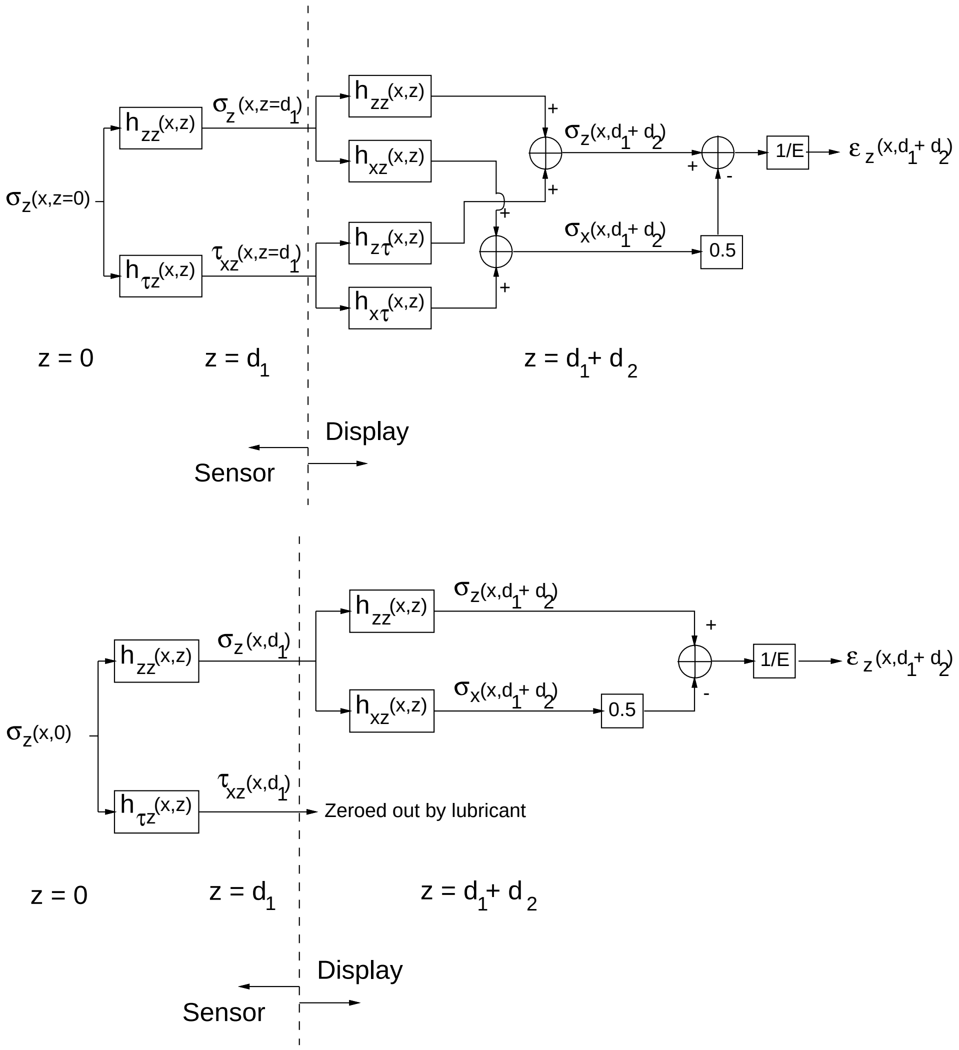

Figure 4: Block diagram representation of the system with two 1 mm sheets of rubber with a) no lubricant, b) a lubricant in between the rubber layers. We assume a frictionless indentation on the surface of the tactile sensor, $\tau_{xz}(x, z = 0) \equiv 0$.

2.2 Block Diagrams and Frequency Responses

For our teletaction model, stimuli are transmitted through two rubber layers to the finger. The two rubber layers represent the tactile sensor and display (Figure 2b). We want to model the normal strain due to indentations from the stimuli with the two different boundary conditions between the rubber layers. In the first case, the rubber layer is two 1 mm sheets of rubber. The block diagram for the first case is represented in Figure 4a. In the second case, we use two 1 mm sheets of rubber with a lubricant between the layers, and this is represented in Figure 4b. This lubricant has the effect of reducing (and in the ideal case, zeroing) the shear stress from the first layer to the second layer. Note that we neglect the boundary conditions between the two layers and always assume an infinite slice.

We assume a normal frictionless indentation, so $\tau_{xz}(x) = 0$ at the contact surface. The relations of the blocks from Figure 4, based on line load equations are:

$$\begin{aligned}
h_{zz}(x,z) &= \frac{-2z^3}{\pi r^4}, H_{zz}(s,z) = -2\pi z e^{-2\pi z s}(\frac{1}{2\pi z} + s), \\
h_{xz}(x,z) &= \frac{-2x^2 z}{\pi r^4}, H_{xz}(s,z) = -2\pi z e^{-2\pi z s}(\frac{1}{2\pi z} - s), \\
h_{\tau z}(x,z) &= \frac{-2xz^2}{\pi r^4}, H_{\tau z}(s,z) = j2\pi z s e^{-2\pi z s}, \\
h_{z\tau}(x,z) &= \frac{-2xz^2}{\pi r^4}, H_{z\tau}(s,z) = j2\pi z s e^{-2\pi z s}, \\
h_{x\tau}(x,z) &= \frac{-2x^2 z}{\pi r^4}, H_{x\tau}(s,z) = j(2 - 2\pi z s)e^{-2\pi z s},
\end{aligned}$$

where z is the depth of interest, $s \geq 0$ is the spatial frequency, and $r^2 = x^2 + z^2$. We assume all layers are half plane and neglect finite thickness.

From the block diagrams and relations, transfer functions are calculated for both systems. With no lubricant between the rubber layers (complete shear stress information transmitted), the overall frequency response for the teletaction system is:

$$\begin{aligned}
H_s(s) &= \frac{\mathcal{F}[\epsilon_z(x, z = d_1 + d_2)]}{\mathcal{F}[\sigma_z(x, z = 0)]} \\
&= \frac{1}{E} e^{-2\pi(d_1+d_2)s}(\frac{1}{2} + 3\pi(d_1 + d_2)s)
\end{aligned}$$

With lubricant between the rubber layers (no shear stress information transmitted), the overall frequency response for the teletaction system is:

$$H_{ns}(s) = \frac{\mathcal{F}[\epsilon_z(x, z = d_1 + d_2)]}{\mathcal{F}[\sigma_z(x, z = 0)]}$$
$$= \frac{1}{E} e^{-2\pi(d_1+d_2)s}(\frac{1}{2} + \pi(d_1 + 3d_2)s + 6\pi^2 d_1 d_2 s^2)$$

In our case, we set $d_1 = 1.0$ mm and $d_2 = 1.7$ mm (1.0 mm for the second rubber layer and 0.7 mm for approximate depth of the mechanoreceptors in the skin). The frequency responses are plotted in Figure 5.

2.3 Surface Stress Profile from Displacement Profiles

The systems above predict the normal strain profile given the input normal stress profile. Since we actually have a displacement profile input from the gratings, we need to find the

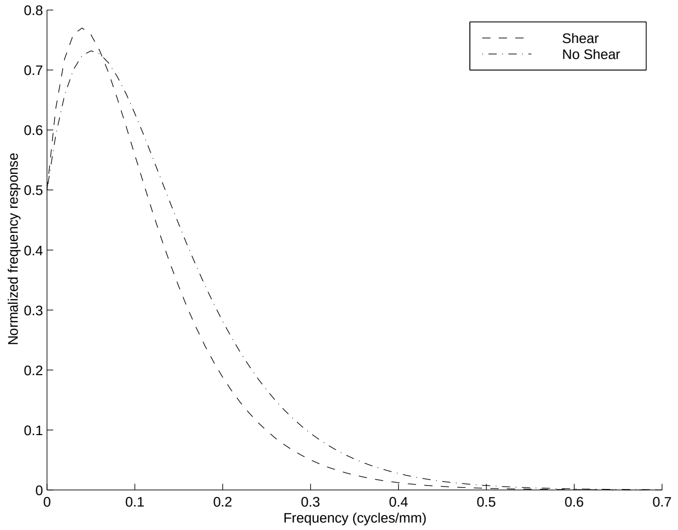

Figure 5: Normalized frequency responses of the block diagrams in Figure 4 when $d_1+d_2 = 2.7$ mm.

equivalent set of line loads corresponding to a given displacement profile. We follow the procedure of [Phillips and Johnson 1981] as detailed in Appendix A.

Given a deflection profile corresponding to a 4.0 mm period grating indenting 2.0 mm, as shown in Figure 6a, we calculate a line load profile that would produce this deflection profile. Knowing that the normal stress should be zero where there is no contact with the grating, and limiting our surface normal stress to only have compressive components, we are left with a surface normal stress profile, $\sigma_z(x)$, shown in Figure 6b. The deflection profile corresponding to $\sigma_z(x)$, shown in Figure 6c, can be found by convolving $\sigma_z(x)$ and $c(x)$, the deflection due to a line load (Appendix A).

2.4 Modulation Index

From the surface normal stress, we can calculate the normal strain profile, $\epsilon_z(x)$, for the two different systems shown in Figure 4. A modulation index is calculated for each of the normal strain profiles. The normal strain profile from -10 mm to 10 mm (to avoid the edge effects) can be approximately represented as

$$\epsilon_z(x) \sim \alpha(1 + \mu \cos(\omega x))$$

where α is a scaling constant, ω is the frequency of the grating, and μ is the modulation index. The two normal strain profiles are shown in Figure 7. As predicted by Figure 5, the modulation index when no shear information is transmitted is higher than when shear

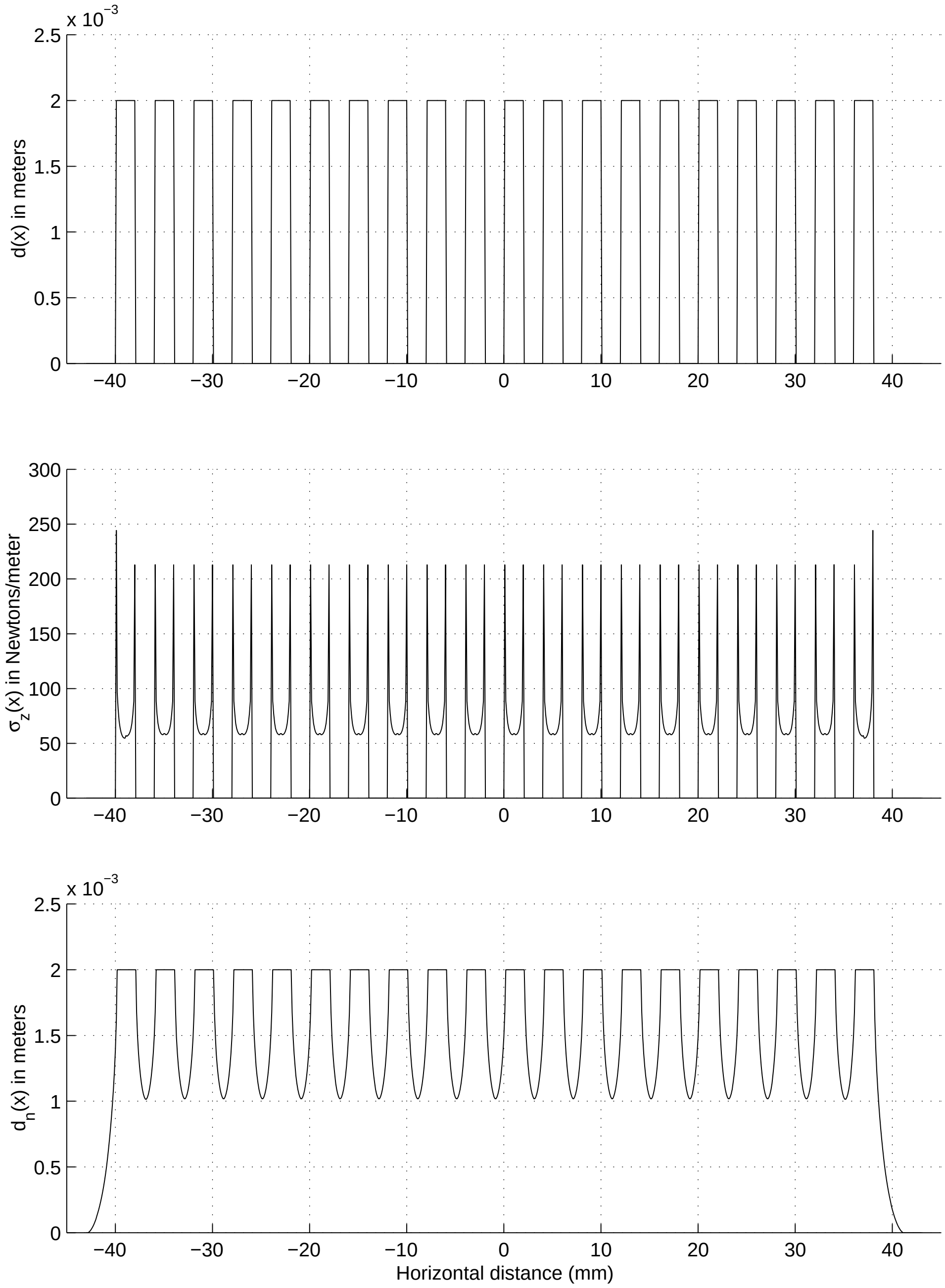

Figure 6: a) Displacement profile applied, b) Surface normal stress, and c) Displacement profile calculated by convolving normal stress in b) with the c(x) of Figure 15.

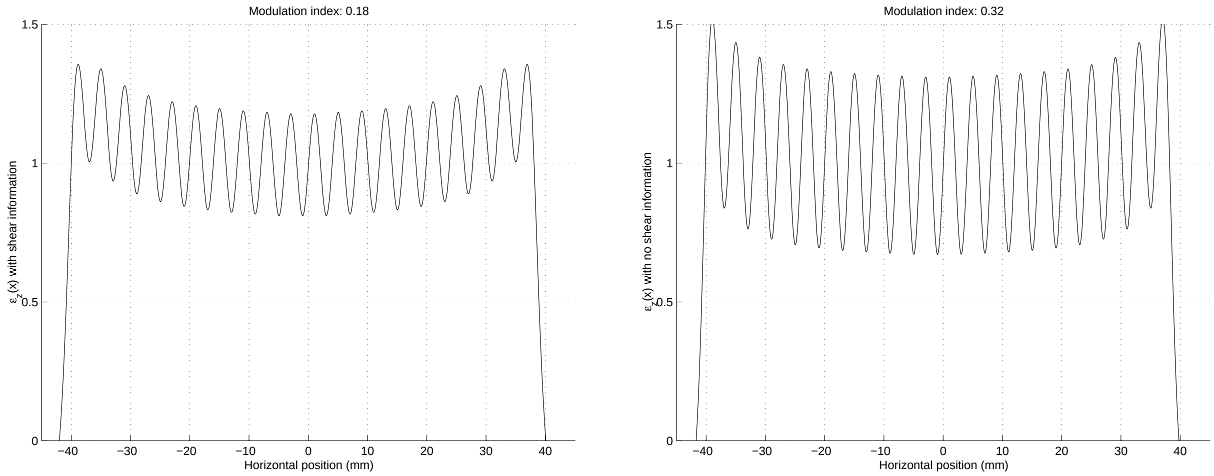

Figure 7: The two normalized normal strains and modulation indices at a depth of 2.7 mm due to a 4.0 mm periodic grating pattern.

information is transmitted. Figure 8 shows the modulation indices as a function of the grating frequency used as input. Note that with a 2 mm low pass layer, the grating frequencies of 0.2 to 0.5 cycles/mm contain information mostly at the fundamental frequency. The higher harmonics are greatly attenuated as shown in the frequency response (Figure 5). With an SA I mechanoreceptor density of 1 mm^{-1}, the highest frequency that can be accurately perceived is a 0.5 cycle/mm grating by the Nyquist sampling criterion.

We assume that each subject has a threshold modulation index. Any grating that has a higher modulation index will be perceived. Theoretically, at a sufficiently high modulation index, all subjects should be able to perfectly perceive the gratings. With lubricated elastic layers, we predict that gratings of the same period will have a higher modulation index. If the increased modulation index exceeds the subject's threshold, then orientation discrimination should be greater than chance. Thus, with lubricated elastic layers, higher frequency gratings should be detected.

2.5 Noise and Distortion

As the modulation index increases, the gratings are more easily perceived. The strain pattern presented to the finger can be thought of as the superposition of the strain from the grating pattern and white noise. At high frequencies, we predict that subjects will not be able to gather any information from the grating since the noise will mask the strain signal. As the grating frequency decreases, the strain signal increases, and the subjects will be able

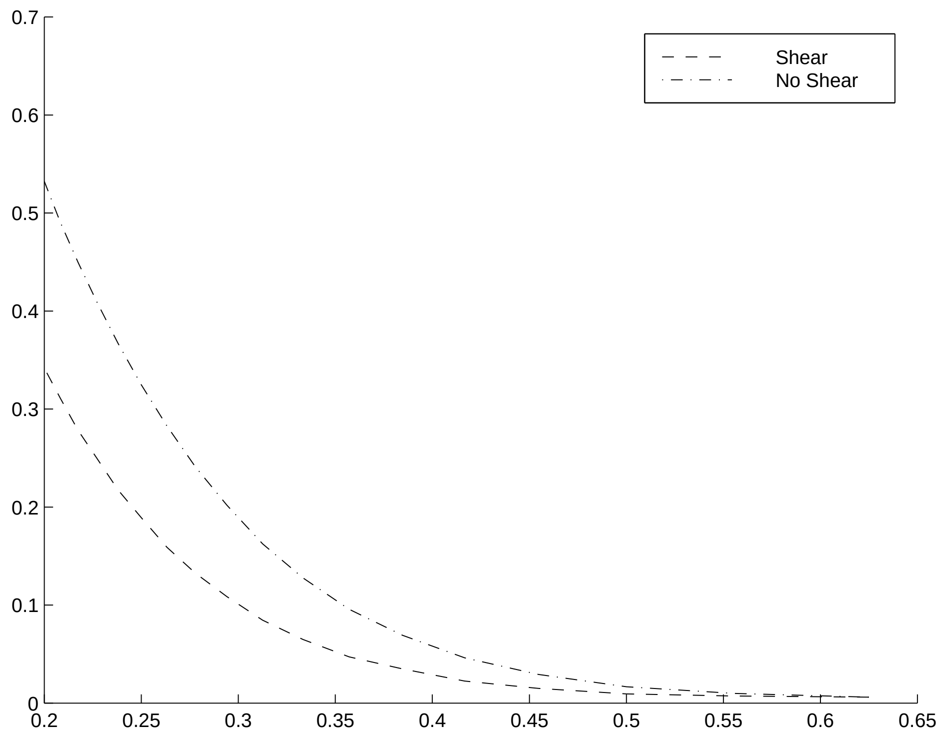

Figure 8: Modulation index vs. frequency.

to gather information about the orientation of the grating. At a sufficiently low grating frequency, all subjects should be able to perfectly determine the grating orientation.

When the lubricant is present between the two layers of rubber, we model the effect as a distortion to the normal strain signal compared to using two layers of rubber without lubrication. This distortion limits the signal to noise ratio (SNR) of the new strain when compared with the normal strain signal using two layers of rubber without lubrication. Figure 9 and Figure 10 show the normal strains with and without shear stress information transmission for various inputs applied normal to the surface and at an angle of 30 degrees to the surface.

We define SNR as follows:

$$SNR = 10log_{10}\left(\frac{\int_{-\infty}^{\infty} \epsilon_{zs}^2(x)dx}{\int_{-\infty}^{\infty}[\epsilon_{zs}(x) - \epsilon_{zns}(x)]^2 dx}\right)$$

where $\epsilon_{zs}(x)$ is the normal strain in the z direction at a depth z without lubrication (shear) and $\epsilon_{zns}(x)$ is the normal strain in the z direction at a depth z with lubrication (no shear).

In the case of gratings applied normally, the normal strain is distorted when shear stress is

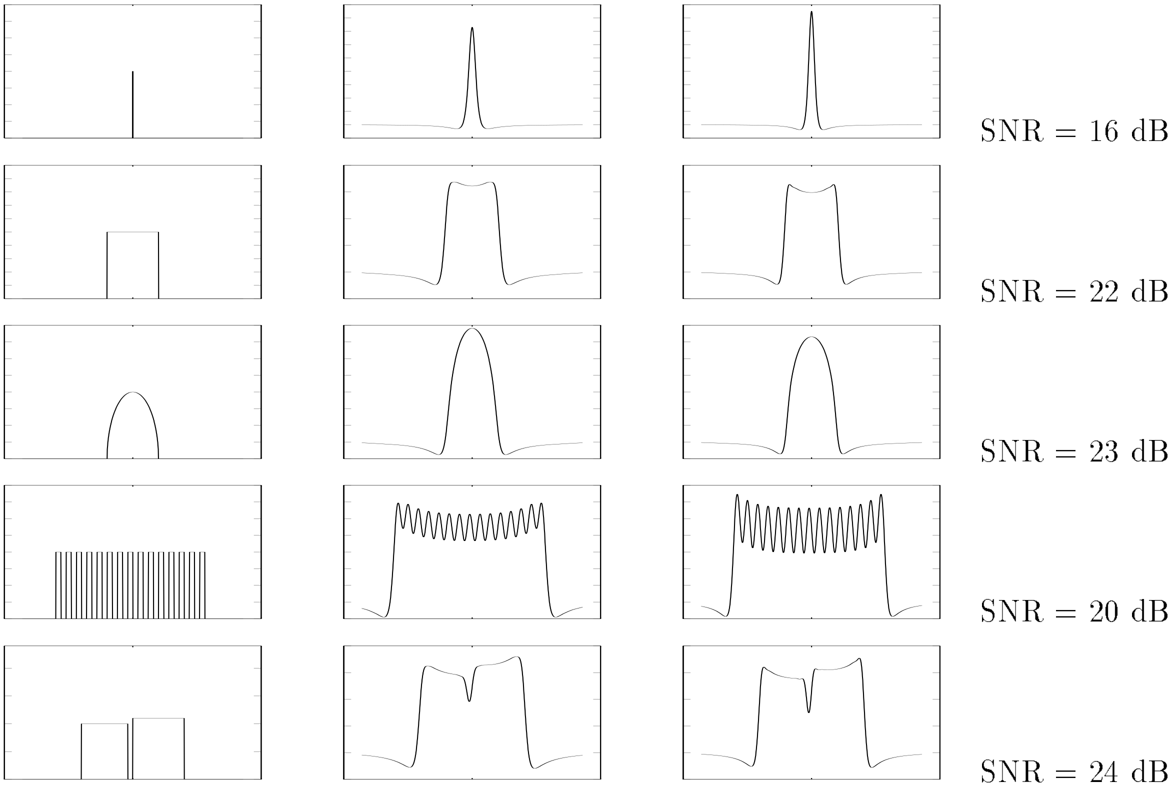

Figure 9: SNR of normal strain without shear information transmission. First column is the displacement input applied normally; Second column is the normal strain with shear information transmission; Third column is the normal strain without shear information transmission. First row is a line load; Second row is a block indenter; Third row is a cylindrical indenter; Fourth row is a grating with 4.0mm period; Fifth row is two block indenters at different heights. Rubber layers have thickness $d_1 = 1.0$ mm and $d_2 = 1.7$ mm.

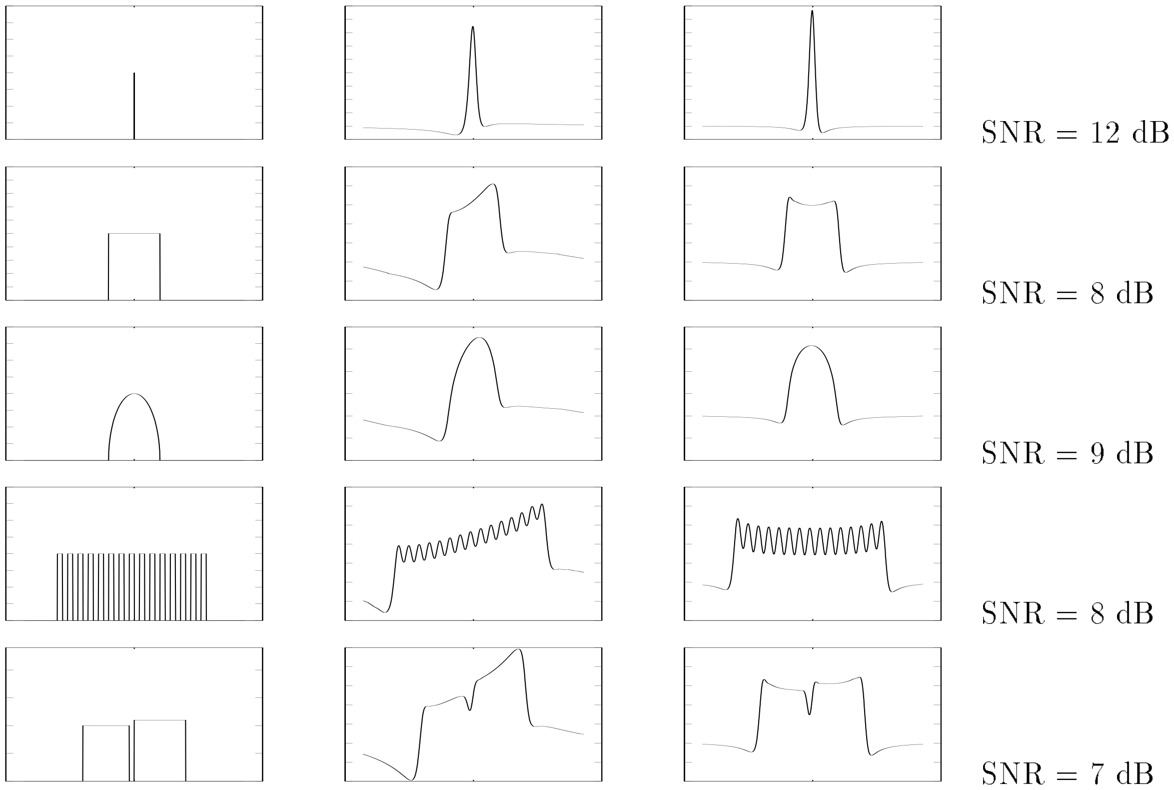

Figure 10: SNR of normal strain without shear information transmission. First column is the displacement input applied at an angle of 30 degrees; Second column is the normal strain with shear information transmission; Third column is the normal strain without shear information transmission. First row is a line load; Second row is a block indenter; Third row is a cylindrical indenter; Fourth row is a grating with 4.0mm period; Fifth row is two block indenters at different heights. Rubber layers have thickness $d_1 = 1.0$ mm and $d_2 = 1.7$ mm.

zeroed, but the modulation index is higher. This leads us to believe that the "noise" caused by the distortion is periodic with the grating period. When the stimuli is applied at an angle, without shear information transmission, almost all information about the tangential forces applied to the surface is lost.

3 Experimental Methods

To test the thresholds of human tactile resolution with and without the transmission of shear stress information, we built a system which presents stimuli with different spatial frequencies and orientations and allows the two different rubber layers to be easily exchanged. The system provides high position control repeatability. The motion control was provided by two motorized linear tables and one motorized rotary table, configured in the x, y, and θ orientation shown in Figure 11a. The motorized tables were controlled by a Pentium based PC running Windows NT 4.0. A control program recorded the subjects' responses.

Two stimuli holders with 10 stimuli were bolted onto the rotary table (Figure 11b). Wax blocks with horizontal or vertical grating patterns were placed into the holders. The grating patterns had periods ranging from 2.4 mm to 4.8 mm in 0.6 mm increments with a 50% duty cycle. This narrow range of periods was based on the results of [Tan 1995]. The rubber layer was either a solid 2 mm silicone rubber sheet or two 1 mm silicone rubber sheets with a thin layer of lubricant in between. We used a vegetable oil spray, PAM[3], as the lubricant as other lubricants we tried either dried up too quickly or reacted unfavorably with the silicone rubber. The 2 mm thickness for the rubber layer was used based on having an actuator array with 2 mm spacing between the actuators. The 1:1 ratio of spacing and layer thickness gives good anti-aliasing characteristics and an acceptable signal to noise ratio.

The subject's right index finger was placed in a position such that the presented stimuli would come into contact normally with the fingerpad. It was essential that no extraneous information was given to the subject by having the stimuli contact obliquely and slide across the finger when coming to the final contact position. Two safety devices were incorporated into the design of the system. An emergency stop button was located in an easily accessible place to immediately stop all motion of the motor tables. The other safety device was a magnetic breakaway located on the finger rest.

[3]American Home Products, Inc.

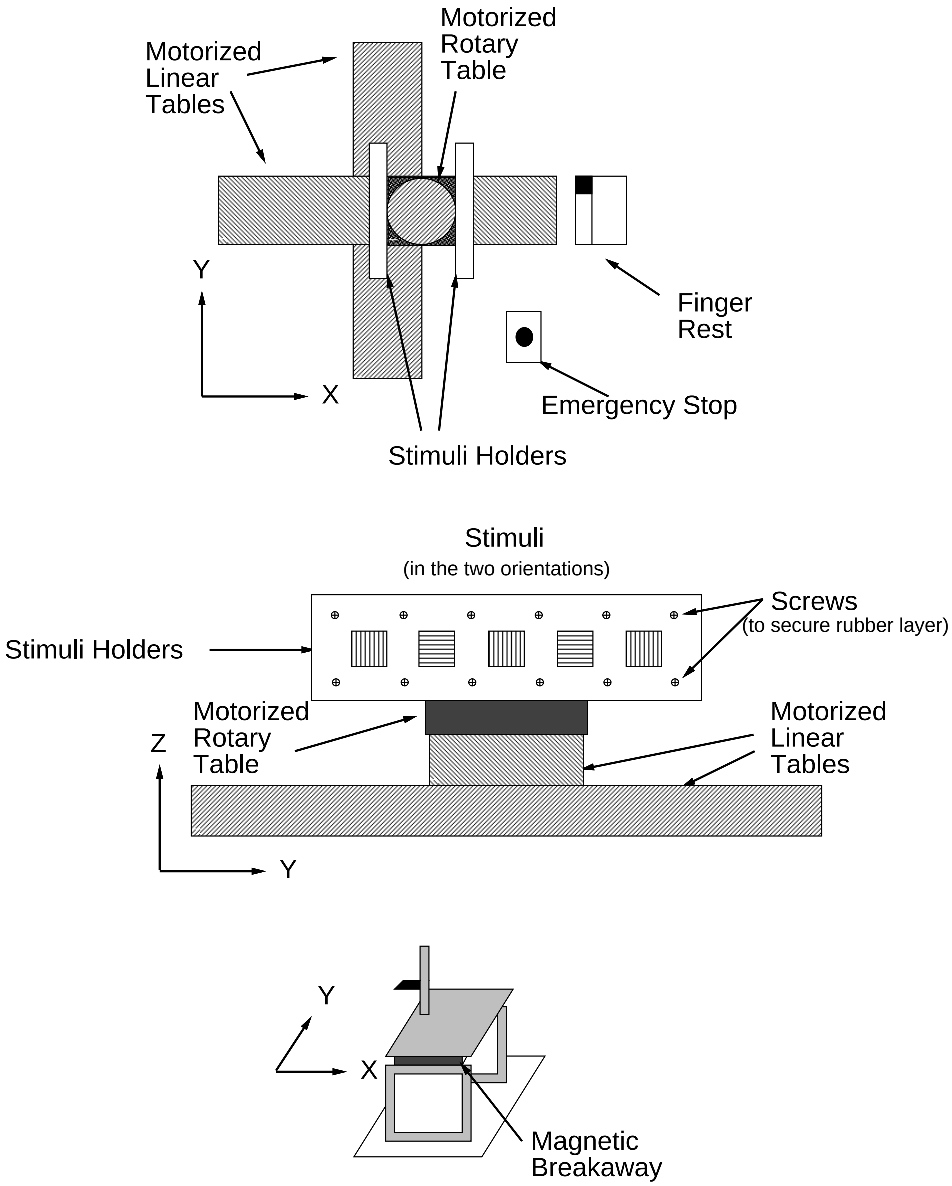

Figure 11: Testing apparatus: a) Top view of overall setup, b) Front view of the tables, stimuli holder, and stimuli, c) Side view of the finger rest

3.1 Procedure

Our goal was to measure change in tactile spatial sensitivity without the transmission of shear stress information. Therefore, we designed experiments that measured the threshold of orientation detection with and without the shear stress information.

The experiment consisted of two trials. For the anti-aliasing spatial low-pass filter, one trial used a solid 2 mm silicone rubber sheet and the other trial used two 1 mm silicone rubber sheets with a thin layer of PAM in between. It was randomly decided which trial was performed first.

In each of the trials, the subject extended their right index finger and placed it on the finger rest (Figure 11c). The finger rest was adjusted to insure that contact with the stimuli would occur in the normal direction of the fingerpad. The control program then allowed the subject to choose how much the stimuli indents into their finger. The setup was calibrated with a dial indicator to insure that each stimulus would indent to the chosen distance with error of less than 25 μm. The subject was allowed to go through ten stimuli to make sure that the correct amount of pressure was applied. If more or less pressure was needed, the system allowed for recalibration to a new displacement. This new displacement was used for the rest of the stimuli in this trial.

The control program then presented each of the ten stimuli fifteen times in a random order. Of the ten stimuli, there were 5 distinct frequencies tested in both orientations. This resulted in thirty points per frequency tested with half of the points in each orientation. Thirty points per frequency were used because the normal distribution is a good approximation, regardless of the shape of the population, if the sample size is greater than or equal to thirty [Walpole and Myers 1972].

After the control program presented the stimuli, the subject responded with a “0” or “1” corresponding to which orientation was felt (Figure 12). The trial was then repeated with the other rubber layer. Each trial took approximately 30 minutes and could be completed on different days, if necessary.

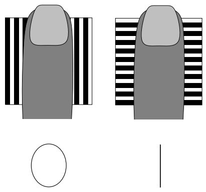

Figure 12: Subjects' response for perceived orientation

Materials	Friction Coeff.
Rubber/wax	1.4
Rubber/Rubber (no lubricant)	2.7
Rubber/Rubber (lubricant)	0.1

Table 2: Measured coefficients of friction

3.2 Friction coefficients

To measure friction coefficients between rubber and wax, a mass was placed on top of the materials being tested. We measured the horizontal force needed to move the rubber which gives the friction coefficient. The test was repeated for two sheets of rubber, with and without the lubricant. As shown in Table 2, there was a significant decrease in friction with the lubricant. The low friction between the lubricated layers corresponded to a reduction of $\tau_{xz}(x, z = d_1)$ applied to the second elastic layer (Figure 4b). We assumed that only the normal stress profile, $\sigma_z(x, z = d_1)$ was transmitted to the second elastic layer.

4 Results

The experiments were run on 10 human subjects (9 male, 1 female). All subjects were volunteers, and two subjects were familiar with the experimental procedure and apparatus. We assume that the subjects are a good representation of the population. The subjects' results are shown in Table 3. The graph of the data averaged over all subjects is shown in Figure 13. Graphs of the data are shown in Figure 14.

Looking at the average of all the subjects (Figure 13), we see that at a 2.4 mm period grating, the percentage correct is approximately chance. As the gratings get more coarse, the percentage correct tends to increase. In the case without shear information transmission, the percentage correct at 4.2 mm and 4.8 mm period gratings was much higher than the

Shear					
Period (mm)	2.4	3.0	3.6	4.2	4.8
Subject 1	40	50	77	93	97
Subject 2	67	53	53	73	87
Subject 3	43	47	37	70	73
Subject 4	57	50	57	77	40
Subject 5	57	50	60	90	77
Subject 6	43	73	60	83	87
Subject 7	43	50	50	60	70
Subject 8	40	60	50	83	90
Subject 9	50	50	67	77	93
Subject 10	23	50	63	60	67
Mean	46	53	57	77	78
95% upper	68	71	76	90	90
95% lower	29	33	36	60	60

Reduced Shear					
Period (mm)	2.4	3.0	3.6	4.2	4.8
Subject 1	40	70	80	87	100
Subject 2	70	50	50	100	97
Subject 3	67	57	50	100	93
Subject 4	57	90	90	90	100
Subject 5	53	60	60	97	100
Subject 6	47	93	70	93	83
Subject 7	50	50	50	87	87
Subject 8	47	47	80	100	97
Subject 9	53	60	77	97	93
Subject 10	43	47	73	87	83
Mean	53	62	68	94	93
95% upper	70	80	84	100	100
95% lower	33	44	53	80	80

Table 3: Raw data from experiments. Numbers are percent correct out of 30 trials per period per subject. The bounds are for a 95% confidence intervals for a proportion (two-sided)

corresponding percentages with shear information.

As seen in Figure 13, the no-shear case has a higher correct percentage at higher spatial periods. We need to determine if the difference is statistically significant. Using 95% confidence intervals for a proportion with 30 samples, we can decide whether the results for the shear and no-shear cases are from the same sample population at each grating period [Natrella 1963]. A normal approximation to a binomial distibution is only valid when both Np and $N(1-p)$ are greater than 5 [Walpole and Myers 1972]. In the 4.2 and 4.8 mm no-shear case, $N(1-p) < 5$.

For grating periods of 2.4 mm, 3.0 mm, and 3.6 mm, the mean of percentage correct for the shear case is inside the 95% interval of the no-shear case, and vice-versa. For grating periods of 4.2 mm and 4.8 mm, the means are outside the 95% intervals of the other case.

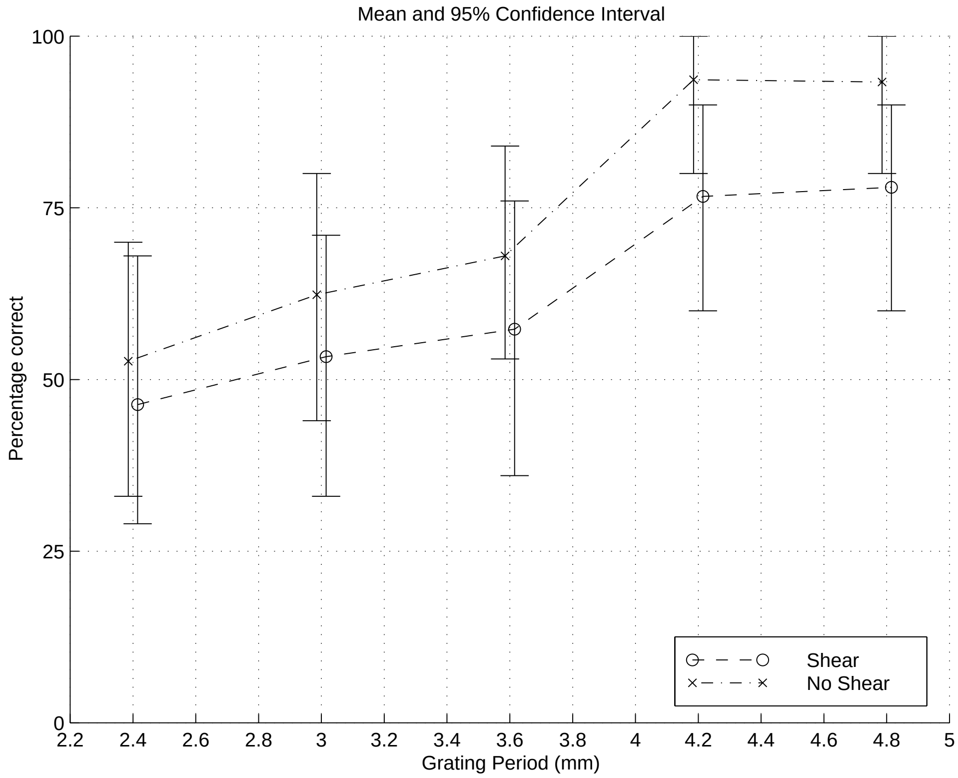

Figure 13: Average of the data and 95% confidence intervals

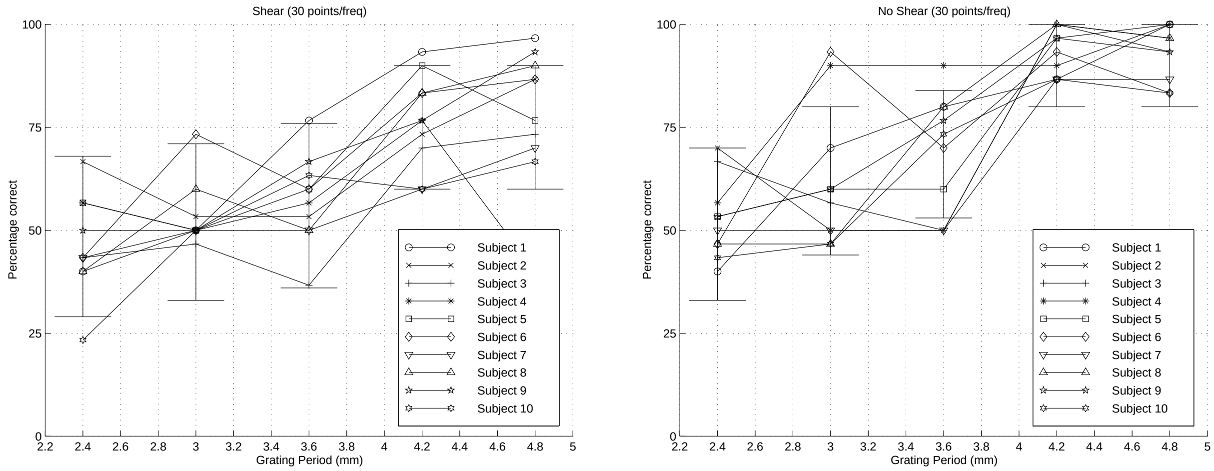

Figure 14: Graphs of the raw data and 95% confidence intervals

From this, we conclude that there is a statistical difference in the 4.2 mm and 4.8 mm cases.

The experiment is designed so that in both the shear and no-shear case, at the 2.4 mm grating period, the responses should be at chance (50%), since 2.4 mm is below the threshold of detectability using a 2mm thickness rubber layer between the finger and stimuli [Tan 1995].

5 Discussion and Conclusion

5.1 Effect of Reducing Shear on Orientation Detection

Looking at just the averages of the raw data, we see that for all grating periods, subjects could more easily discriminate the orientation of the stimuli with reduced shear stress. Instead of a 76-78% correct response rate for the full shear transmission case, there is a 93-94% correct response rate for the reduced shear transmission case with stimuli of period 4.2 mm and 4.8 mm. Assuming that the correct response rate is an increasing function with respect to stimuli period, there should be an increase in spatial resolution.

5.2 Effect on Tactile Display Design

The increase in spatial resolution without shear stress information being transmitted can be best explained by the increase in the modulation index for the frequencies of interest (Figure 8). When shear is removed in the intermediate boundary, the model predicts an increase in modulation indices, and the experiments confirms that at the frequencies tested, the percentage correct was always greater when there was no shear stress information transmitted between the elastic layers.

If we assume that each subject has a threshold period, then the tactile spatial resolution should be improved by reducing the shear stress information. This idea is put to practice in the Sensopad®, a device which aids in breast self examinations. It is constructed by placing silicone fluid in between two layers of silicone rubber. Its claim of enhancing the perception of small embedded objects agrees with our results.

In previous work, we compared the normal subsurface strain with and without shear information transmitted at the boundary layer [Fearing et al 1997]. We found that the distortion caused by removing shear information caused a 16dB discrepancy between the strain profiles for a normal line load and 20dB for a grating. This distortion apparently increased the modulation index for gratings, which told us that the discrepancy amplified the periodic components of the normal strain profile. Shear information might be important in sensing and reconstructing other types of contacts, such as a cylindrical indenter or an angled indentation, but not normal frictionless contacts.

In designing a teletaction system, it is important to consider what type of contacts the sensor will encounter. If the sensor operates in an environment where contact is composed of mainly normal stresses, the reduction of shear stress information can be beneficial by enhancing the higher frequency information present in subsurface skin strain. An example of such an environment is laparoscopic surgery with tactile sensors on the ends of the instruments. Contact with organs will be low friction contacts due to the slipperiness of the organs. This leads to a contact where normal stresses are high compared to tangential stresses. In these environments, a tactile display using an array of 1 DOF actuators should be as effective as using an array of 3 DOF actuators. From the model and data, an array of 1 DOF actuators displaying a normal stress pattern has a higher modulation index than an array of 3 DOF actuators displaying the corresponding normal and shear stress patterns.

5.3 Sources of Error

Some inconsistencies in the data might have been due to weaknesses in the apparatus. Using a force controlled apparatus would probably have given more consistent stimuli indentation pressures than a position controlled apparatus. Without any force feedback, we were not able to insure the same stimuli indentation pressure between subjects. For comfort, the apparatus did not have a finger restraint, so additional information might have been perceived by the finger if the subject moved his or her finger around when in contact with the stimuli. Additional inconsistencies could occur from hysteresis of the finger, fatigue of the subject, vibration or slip of the stimuli. Extra information perceived by the subject due to vibration or slip could inadvertently skew the data towards the no-shear case, since slippage more easily occurred when there was a lubricant between the elastic layers. We used a 95% confidence interval for a proportion which has a large sampled mean variation. Having more trials per subject would reduce the variation, but increase fatigue or other factors if too many trials were performed in a row.

The model we used is very simplistic when compared to what really occurs in the mechanoreceptors and finger. We also assumed that the skin and rubber formed one continuous layer and had the same elastic modulus.

6 Future Work

In our experiments, we constrained the finger to be static with respect to the stimuli. Future work includes allowing subjects to scan the stimuli, to simulate more realistic searching and scanning methods. We will also use better models of the finger/elastic layer/stimuli interaction, and testing stimuli with a tangential stress component. Refinement of our apparatus will include integrating a force/torque sensor to give a more consistent presentation of stimuli.

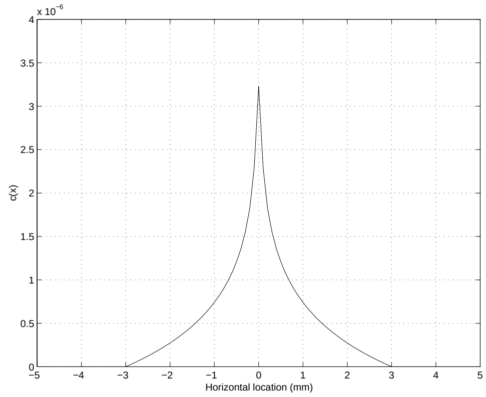

Figure 15: Deflection profile, c(x), caused by a line load at $x = 0$ with $x_0 = 25\,\mu$ m and $x_b = 3.0$ mm

Appendix A

Determining Surface Stresses from a Deflection Profile

In planar elasticity, the basic relation between a surface deflection and a normally applied line load is shown in Figure 15, and given by:

$$c(x) = \begin{cases} \frac{2}{\pi E} log \frac{x_b}{x_o}, & |x| < x_o \\ \frac{2}{\pi E} log \frac{x_b}{x}, & x_o < |x| < x_b \\ 0, & x_b < |x| \end{cases} \tag{1}$$

where x_0 is half the width of the applied line load, and x_b is a distant boundary. From equation 1, the line load has a constant deflection in the width of application, decays logarithmically until the distant boundary, and is zero outside of the distant boundary. We used the same values as [Phillips and Johnson 1981] and [Tan 1995], $x_0 = 25\ \mu$m and $x_b = 3$ mm.

As in [Phillips and Johnson 1981], we assume that the deflection is proportional to the magnitude of the line load, the deflection function c(x) is space invariant, and the overall deflection profile is the superposition of deflection profiles from the individual line loads. Discretizing c(x), we can represent the discretized deflection profile d(x_i) as:

$$d(x_i) = \sum_{j=1}^{n} c(x_i - x_j)p(x_j) \tag{2}$$

where $p(x_j)$ is the discretized line load profile, and n is the number of points representing the profiles. Rewriting equation 2 least squares problem. Given a deflection profile d and the deflection matrix C (calculated from c(x)), we can find p as follows:

$$Cp = d \tag{3}$$

$$p = (C^T C)^{-1} C^T d \tag{4}$$

In our case, p and d are the same length, so

$$p = C^{-1} d \tag{5}$$

Appendix B

Matlab code for Elastic Half Plane Models

This is the Matlab code for the model.

```
::::::::::::::
doit.m
::::::::::::::
mods = [];
mods2 = [];
for t=1.6:.2:5.0
  init
  test2n
  m3 = modulationindex(ep2, x, 10);
  mm3 = modind2(ep2,x,10);
%  test2h
%  m2 = modulationindex(ep2, x, 10);
%  mm2 = modind2(ep2,x,10);
m2 = 0;
mm2 = 0;
  test
  m1 = modulationindex(ep, x, 10);
  mm1 = modind2(ep,x,10);

  mods = [mods; [t m1 m2 m3]];
  mods2 = [mods2; [t mm1 mm2 mm3]];


 [t m1 mm1 m2 mm2 m3 mm3]
end

save modindex mods
save modindex2 mods2

figure
hold on
x = 1./mods(:,1);
plot(x, (mods(:,2)),'--');
%plot(x, (mods(:,3)));
plot(x, (mods(:,4)),'-.');
legend('Shear','No Shear');

figure
hold on
x = 1./mods2(:,1);
plot(x, (mods2(:,2)),'--');
%plot(x, (mods2(:,3)));
plot(x, (mods2(:,4)),'-.');
legend('Shear','No Shear');

::::::::::::::
init.m
::::::::::::::
delx = .1;           % discretization period (in mm)
z1 = 1;             % depth of interest (in mm)
z2 = 1.7;
edgeofforces = 43;  % where range of forces is allowed (in mm)

x = [-edgeofforces:delx:edgeofforces];
l = length(x);
q = zeros(1,l);
d = zeros(1,l);
maxx = (find(x == edgeofforces - 13));   % buffer zones to see edge effects
midx = (find(x == 0));
```

```
minx = (find(x == -edgeofforces + 13));

% *** square wave ***
%t = 4.0;  % spacing (period of grating)
n = round(t/delx);
n2 = round(t/2/delx);
for i=1:floor((maxx-minx)/n)
 d((i-1)*n+1+minx:(i-1)*n+n2+minx) = ones(1,n2) * 2e-3;
end

% *** block indentor ***
%d(minx:maxx) = ones(1,maxx-minx+1) * 1e-3;
%d(minx:midx) = ones(1,midx-minx+1) * 2e-3;

% *** cylindrical indentor ***
%d(minx:maxx) = sqrt(x(maxx)^2 - x(minx:maxx).^2) * 2e-3 / x(maxx);

% *** line load ***
%d(find(x == 0)) = 2e-3;

[p d1] = surfacestress(d, x);
%q = 0.5*p;
in1=[p; q; x];

clear minx maxx n n2 i edgeofforces l p q x delx

d1 = d1((length(d1)-1)/4:3*(length(d1)-1)/4);
::::::::::::::
modind2.m
::::::::::::::
function m = modind2(ep,x,edg)

a = find(x == -edg);
b = find(x == edg);
ep = ep(a:b);
m = (max(ep)-min(ep))/(max(ep)+min(ep));
::::::::::::::
modulationindex.m
::::::::::::::
function m = modulationindex(ep,x,edg)

a = find(x == -edg);
b = find(x == edg);
ep = ep(a:b);
l = length(ep);
max1 = ep(2:l-1) > ep(1:l-2);
max2 = ep(2:l-1) > ep(3:l);
max3 = max1 + max2;
maxs = find(max3 == 2);
maxav = mean(ep(maxs));

min1 = ep(2:l-1) < ep(1:l-2);
min2 = ep(2:l-1) < ep(3:l);
min3 = min1 + min2;
mins = find(min3 == 2);
minav = mean(ep(mins));

av = mean(ep);
%av = mean(ep(maxs(1):maxs(length(maxs))));

m = [(maxav-minav)/av/2];
::::::::::::::
plotall.m
::::::::::::::
function plotall(x,sz,sx,txz,ep)

figure
subplot(4,1,1);
```

```
plot(x,sz);
subplot(4,1,2);
plot(x,sx);
subplot(4,1,3);
plot(x,txz);
subplot(4,1,4);
plot(x,ep);
::::::::::::::
plotit.m
::::::::::::::
function snr = plotit(x, stimuli, ep1, ep2, maxx)

a = find(x == -5);
b = find(x == 5);

x = x(a:b);
ep1 = ep1(a:b);
ep2 = ep2(a:b);
snr = 10 * log10(norm(ep1)^2/norm(ep1-ep2)^2);

figure
subplot(3,1,1)
plot(x,ep1)
ylabel('First');
subplot(3,1,2)
plot(x,ep2)
ylabel('Second');
subplot(3,1,3)
plot(x,ep1-ep2)
ylabel('1st-2nd');
st = sprintf('%5.3f',snr);
xlabel(st)

::::::::::::::
shears2.m
::::::::::::::
function [sigz, sigx, txz] = shears2(z,in)
% Calculate normal and shear stresses at a depth z with
% surface stress in(1,:)
% surface shear  in(2,:)
% range          in(3,:)

% error checking
if size(in,2) == 3
 in = in'
end

% some more initialization
P = in(1,:);   % normal loads
Q = in(2,:);   % tangential loads
x = in(3,:);
l = length(x);
delx = (max(x)-min(x))/(l-1);
a = find(x == 0);

den = pi*(x.^2 + z^2).^2;

hzz = (2*z^3)./den;
hzx = (2*(z^2).*x)./den;
hxz = (2*z).*(x.^2)./den;
hxx = (2*x.^3)./den;
tz  = (2*(z^2).*x)./den;
tx  = (2*z).*(x.^2)./den;

Hzz = toeplitz([hzz(a:-1:1), zeros(1,a-1)],[hzz(a:l) zeros(1,a-1)]);
Hzx = toeplitz([hzx(a:-1:1), zeros(1,a-1)],[hzx(a:l) zeros(1,a-1)]);
Hxz = toeplitz([hxz(a:-1:1), zeros(1,a-1)],[hxz(a:l) zeros(1,a-1)]);
Hxx = toeplitz([hxx(a:-1:1), zeros(1,a-1)],[hxx(a:l) zeros(1,a-1)]);
```

```
Tz  = toeplitz([tz(a:-1:1),  zeros(1,a-1)],[tz(a:1) zeros(1,a-1)]);
Tx  = toeplitz([tx(a:-1:1),  zeros(1,a-1)],[tx(a:1) zeros(1,a-1)]);

sigz = [Hzz*P' + Hzx*Q']' * delx;
sigx = [Hxx*Q' + Hxz*P']' * delx;
txz =  [Tz*P' + Tx*Q']' * delx;

::::::::::::::
snr.m
::::::::::::::
init
test2n
test
err = sum(ep.^2)/sum((ep - ep2).^2);
s = 10*log10(err);
figure
subplot(1,3,1)
plot(x,d)
tt=sprintf('SNR for noshear = %3.2f',s)
y = get(gca, 'ylim');
xx = get(gca, 'xlim');
set(gca, 'yticklabel', []);
set(gca, 'xticklabel', []);
axis([xx y(1) 2*y(2)]);
subplot(1,3,2)
plot(x,ep)
set(gca, 'yticklabel', []);
set(gca, 'xticklabel', []);
y1 = get(gca, 'ylim');
subplot(1,3,3)
plot(x,ep2)
set(gca, 'yticklabel', []);
set(gca, 'xticklabel', []);
y2 = get(gca, 'ylim');

if (y2(2)>y1(2))
 subplot(1,3,2)
 axis([xx y2])
else
 subplot(1,3,3)
 axis([xx y1])
end
::::::::::::::
snr2.m
::::::::::::::
ss = [];
for t=1.6:.2:8.0
 snr
 ss = [ss, s];
 [t,s]
 close
end

ss = [1.6:.2:5.0; ss];
save snrfreq ss
::::::::::::::
surfacestress.m
::::::::::::::
function [Pnew, Dnew] = surfacestress(D, x)

% Pnew: 1xn of pressure distributions correlating with the displacement
%       profile D
% Dnew: resultant displacement file if Pnew was applied
% D:    1xn of the displacement profile
% x:    the range of locations of interest

D = D';  % Make it a vertical vector
```

```
% Find out spacing
left = min(x);
right = max(x);
delx = (right - left)/(length(x)-1);

yb = 3;     %  3 mm
yo = 25e-3; % 25 um
E = 4.1e5;  % Modulus of elasticity of the rubber

axisi = left:delx:right;
n = length(axisi);

%create response c
c = zeros(1, n);

a = find(abs(axisi) < abs(yo));
c(a) = ones(1,length(a)) * 2/pi/E*log10(abs(yb)/abs(yo));
mina = min(a);
maxa = max(a);

b = find(abs(axisi) < abs(yb));
minb = min(b);
maxb = max(b);
c(minb:mina-1) = 2/pi/E*log10(abs(yb)./abs(axisi(minb:mina-1)));
c(maxa+1:maxb) = 2/pi/E*log10(abs(yb)./abs(axisi(maxa+1:maxb)));

%plot(axisi, c);
clear a b mina maxa minb minb

%create matrix C
a = find(axisi == 0);
C = toeplitz([c(a:length(c)) zeros(1,a-1)]);

temp = find(D ~= 0);
C2 = C(temp,temp);
D2 = D(temp);
P = inv(C2)*D2;
Pnew = zeros(n,1);
Pnew(temp) = P;
Dnew = conv(c,Pnew);

Dnew = Dnew';
Pnew = Pnew';

::::::::::::::
test.m
::::::::::::::
x = in1(3,:);

[sz, sx, txz] = shears2(z1 + z2,in1);
ep = sz - 0.5*sx;
::::::::::::::
test2n.m
::::::::::::::
x = in1(3,:);

[sz, sx, txz] = shears2(z1,in1);
txz = 0 * txz;
ep = sz - 0.5*sx;

in2 = [sz; txz; x];
[sz2, sx2, txz2] = shears2(z2,in2);
ep2 = sz2 - 0.5*sx2;
::::::::::::::
transfer.m
::::::::::::::
z=2;
s=0:.001:1;
```

```
a = find(s == 0);

H1=exp(-4*pi*z/2.*abs(s)).*(0.5 + 6*z/2*pi.*abs(s));
H2=exp(-4*pi*z/2.*abs(s)).*(0.5 + 4*z/2*pi.*abs(s) + 6*(z/2*pi.*abs(s)).^2);

figure
hold on
plot(s,H1,'--');
plot(s,H2,'-.');
legend('shear','no shear');
title('Frequency Response: normal strain/normal stress');
xlabel('freq (cycles/mm)');

figure
hold on
plot(1./s,H1,'--');
plot(1./s,H2,'-.');
axis([1 10 0 0.8]);
legend('shear','no shear');
title('Frequency Response: normal strain/normal stress');
xlabel('period (mm/cycle)');

h1 = ifft(H1);
h2 = ifft(H2);
```

Appendix C

Control Program

This program was compiled under Microsoft Visual C++ 5.0 under Windows NT 4.0 Service Pack 1.

```
#include <windows.h>
#include <stdlib.h>
#include <string.h>
#include <stdio.h>
#include <conio.h>
#include <process.h>
#include <math.h>
#include <time.h>

#include "dmccom.h"

#define  cnts 800   /* Counts per mm */
#define  deg 500   /* Counts per degree */
#define  mm2i   25.4  /* mm per inch */
#define  MaxHSP  40000 /* Maximum counts per second when finding initial position */
#define  MaxXSP 400000 /* Maximum counts per second */
#define  MinXSP  32000 /* counts per second to use in bad motor */
#define  MaxYSP 400000 /* Maximum counts per second */
#define  MaxZSP 200000 /* Maximum counts per second */

void main(void);
void ClearScreen(void);
void DisplayError(long rc);
long bit(long i, long flags);
void initpos(HANDLEDMC hdmc);
void randpos(long pos[10]);
void doit(HANDLEDMC hdmc, long indent, long pos[10]);
long findindent(HANDLEDMC hdmc);

HANDLE  hConsoleOut;                   /* Handle to the console */
CONSOLE_SCREEN_BUFFER_INFO csbiInfo;   /* Console information */
FILE *out;           /* Data File */
int iRow = 0;
double offset[10];

void main()                            /* Thread One */
{
 long   rc;
 char   szMsg[80];
 char   szResponse[32];
 COORD   Coord;
 DWORD   Dummy;
 HANDLEDMC  hdmc;
 long   pos[10];
 long   indent;
 int    subject, trial, i;
 char   resp, filename[13];
 double   offset2[10];
 FILE   *f1;

offset[0] = -0.036;
offset[1] = -0.030;
offset[2] =  0.000;
offset[3] =  0.041;
offset[4] =  0.079;
offset[5] =  0.085;
offset[6] =  0.055;
offset[7] =  0.035;
```

```
offset[8] =  0.020;
offset[9] =  0.013;

/* Add in additional offsets */
f1 = fopen("offsets", "r");
for (i=0; i<10; i++)
{
 fscanf(f1, "%lf\n", &offset2[i]);
 offset[i] += offset2[i];
}
fclose(f1);

/* Get display screen information & clear the screen */
hConsoleOut = GetStdHandle(STD_OUTPUT_HANDLE);
GetConsoleScreenBufferInfo(hConsoleOut, &csbiInfo);
ClearScreen();
SetConsoleTitle("Tactile Experiment");

/* Open the controller */
rc = DMCOpen(1, NULL, &hdmc);
if (rc) DisplayError(rc);

/* Reset, Servo Here, Set Max Speeds, Offset Error */
rc = DMCCommand(hdmc, "RS", szResponse, sizeof(szResponse));
if (rc) DisplayError(rc);
rc = DMCCommand(hdmc, "SH", szResponse, sizeof(szResponse));
if (rc) DisplayError(rc);
rc = DMCCommand(hdmc, "ER 2000,2000,2000", szResponse, sizeof(szResponse));
if (rc) DisplayError(rc);
rc = DMCCommand(hdmc, "OE 1,1,1", szResponse, sizeof(szResponse));
if (rc) DisplayError(rc);

sprintf(szMsg, "SP %ld,%ld,%ld", MaxHSP, MaxHSP, MaxHSP);
rc = DMCCommand(hdmc, szMsg, szResponse, sizeof(szResponse));
if (rc) DisplayError(rc);

/* Go to the initial position */
initpos(hdmc);

/* Set to new Max Speed */
sprintf(szMsg, "SP %ld,%ld,%ld", MaxXSP, MaxYSP, MaxZSP);
rc = DMCCommand(hdmc, szMsg, szResponse, sizeof(szResponse));
if (rc) DisplayError(rc);

/* Creat filename for data collection */
ClearScreen(); iRow = 0;
sprintf(szMsg, "Subject #:");
Coord.X = 0;Coord.Y = iRow;iRow ++;
WriteConsoleOutputCharacter(hConsoleOut, szMsg, strlen(szMsg), Coord, &Dummy);
scanf("%d", &subject);
sprintf(szMsg, "Trial #:");
Coord.X = 0;Coord.Y = iRow;iRow ++;
WriteConsoleOutputCharacter(hConsoleOut, szMsg, strlen(szMsg), Coord, &Dummy);
scanf("%d", &trial);

/* Find correct indentation */
indent = findindent(hdmc);

resp = '\0';

do
{
 if (trial < 10)
  sprintf(filename, "data%d.0%d\0", subject, trial);
 else
  sprintf(filename, "data%d.%d\0", subject, trial);
 Coord.X = 0;Coord.Y = iRow;iRow ++;
 WriteConsoleOutputCharacter(hConsoleOut, filename, strlen(filename), Coord, &Dummy);
```

```
 out = fopen(filename, "w");

 /* Randomize trials and doit */
 randpos(pos);
 doit(hdmc, indent, pos);
 fclose(out);

 ClearScreen(); iRow = 0;
 sprintf(szMsg, "Continue to next trial? (y or n)");
 Coord.X = 0;Coord.Y = iRow;iRow ++;
 WriteConsoleOutputCharacter(hConsoleOut, szMsg, strlen(szMsg), Coord, &Dummy);
 do
 {
  while (!_kbhit()) {}
  resp = _getch();
 }
 while ((resp != 'n') && (resp != 'y'));

 if (resp == 'y')
  trial++;
}
while (resp == 'y');

/* Close the controller */
rc = DMCClose(hdmc);
if (rc) DisplayError(rc);

/* Pause briefly so that the user can read the messages */
// Sleep(2000);

/* Clean up handles */
CloseHandle(hConsoleOut);
}

void ClearScreen(void)
{
   DWORD    Dummy;
   COORD    Home = {0, 0};

   FillConsoleOutputCharacter(hConsoleOut, ' ', csbiInfo.dwSize.X * csbiInfo.dwSize.Y, Home, &Dummy);
}

void DisplayError(long rc)
{
 char  szMsg[80];
   DWORD    Dummy;
   COORD    Coord;

 Coord.X = 0;
 Coord.Y = iRow;
 iRow ++;
 sprintf(szMsg, "Communications error. Return code = %ld.", rc);
 WriteConsoleOutputCharacter(hConsoleOut, szMsg, strlen(szMsg), Coord, &Dummy);
 exit(rc);
}

long bit(long i, long flags)
{
 return((long)((flags/((long)(pow(2,i)))) % 2));
}


void initpos(HANDLEDMC hdmc)
{
 long   rc;
 char   szMsg[80];
 char   szResponse[32];
 COORD   Coord;
```

```
 DWORD   Dummy;
 long   ts[3];

 /* Get Status of Switches */
 rc = DMCCommand(hdmc, "TS", szResponse, sizeof(szResponse));
 if (rc) DisplayError(rc);
 sscanf(szResponse, "%ld, %ld, %ld", &ts[0], &ts[1], &ts[2]);
 sprintf(szMsg, "%ld %ld %ld", ts[0], ts[1], ts[2]);
 Coord.X = 0;Coord.Y = iRow;iRow ++;
 WriteConsoleOutputCharacter(hConsoleOut, szMsg, strlen(szMsg), Coord, &Dummy);

 if ((bit(2,ts[0]) + bit(2,ts[1])) < 2)
 {
  /* Move out a little bit */
  rc = DMCCommand(hdmc, "PR 20000,20000;BG X,Y", szResponse, sizeof(szResponse));
  if (rc) DisplayError(rc);
  rc = DMCWaitForMotionComplete(hdmc, "XY", FALSE);
  if (rc) DisplayError(rc);
 }

 /* Get Status of Switches */
 rc = DMCCommand(hdmc, "TS", szResponse, sizeof(szResponse));
 if (rc) DisplayError(rc);
 sscanf(szResponse, "%ld, %ld, %ld", &ts[0], &ts[1], &ts[2]);
 sprintf(szMsg, "%ld %ld %ld", ts[0], ts[1], ts[2]);
 Coord.X = 0;Coord.Y = iRow;iRow ++;
 WriteConsoleOutputCharacter(hConsoleOut, szMsg, strlen(szMsg), Coord, &Dummy);

 /* Go to Xlimit, Ylimit, ZHome */
 if (bit(2,ts[0]))
 {
  rc = DMCCommand(hdmc, "PR -160000;BGX", szResponse, sizeof(szResponse));
  if (rc) DisplayError(rc);
  rc = DMCWaitForMotionComplete(hdmc, "X", FALSE);
  if (rc) DisplayError(rc);
 }

 if (bit(2,ts[1]))
 {
  rc = DMCCommand(hdmc, "PR ,-160000;BGY", szResponse, sizeof(szResponse));
  if (rc) DisplayError(rc);
  rc = DMCWaitForMotionComplete(hdmc, "Y", FALSE);
  if (rc) DisplayError(rc);
 }

 rc = DMCCommand(hdmc, "HMZ;BGZ", szResponse, sizeof(szResponse));
 if (rc) DisplayError(rc);
 rc = DMCWaitForMotionComplete(hdmc, "Z", FALSE);
 if (rc) DisplayError(rc);

 /* Goto Initial Position */
 sprintf(szMsg, "PR %ld,%ld,%ld;BG X,Y,Z", (long)(2.02*mm2i*cnts),(long)(4.02*mm2i*cnts),-59*deg);
 rc = DMCCommand(hdmc, szMsg, szResponse, sizeof(szResponse));
 if (rc) DisplayError(rc);
 rc = DMCWaitForMotionComplete(hdmc, "XYZ", FALSE);
 if (rc) DisplayError(rc);

 /* Set position as (0,0,0) */
 rc = DMCCommand(hdmc, "DP 0,0,0", szResponse, sizeof(szResponse));
 if (rc) DisplayError(rc);
}

void randpos(long pos[10])
{
 long a,b,c;
 int  i;
```

```
 for (i=0; i<10; i++)
  pos[i] = i+1;

 srand((unsigned)time( NULL ));
 for (i=1; i <= 100; i++)
 {
  a = rand() % 10;
  b = rand() % 10;
  c = pos[a];
  pos[a] = pos[b];
  pos[b] = c;
 }
}

void doit(HANDLEDMC hdmc, long indent, long pos[10])
{
 int    i,a;
 long   rot, lin;
 int    side; /* which side of stimuli to use */
 int    disp; /* displacement away from center */
 char   resp; /* response from user */
 long   rc;
 char   szMsg[80];
 char   szResponse[32];
 COORD   Coord;
    DWORD   Dummy;
// long   tp[3];

 for (i=0; i<10; i++)
 {
  side = (pos[i] > 5);
  disp = (pos[i] - side*5) - 3;
  srand((unsigned)time( NULL ));
  a = 2*side - 1;
  rot = 90*deg;
  lin = (long)(2*disp*cnts*mm2i);

  ClearScreen(); iRow = 0;

  /* Get Position */
/*
  rc = DMCCommand(hdmc, "TP", szResponse, sizeof(szResponse));
  if (rc) DisplayError(rc);
  sscanf(szResponse, "%ld, %ld, %ld", &tp[0], &tp[1], &tp[2]);
  sprintf(szMsg, "%ld %ld %ld", tp[0], tp[1], tp[2]);
  Coord.X = 0;Coord.Y = iRow;iRow ++;
  WriteConsoleOutputCharacter(hConsoleOut, szMsg, strlen(szMsg), Coord, &Dummy);
*/
  sprintf(szMsg, "PR ,%ld,%ld;BG Y,Z", lin,rot);
  rc = DMCCommand(hdmc, szMsg, szResponse, sizeof(szResponse));
  if (rc) DisplayError(rc);
  rc = DMCWaitForMotionComplete(hdmc, "YZ", FALSE);
  if (rc) DisplayError(rc);

  sprintf(szMsg, "PR ,,%ld;BG Z", (long)(a*rot));
  rc = DMCCommand(hdmc, szMsg, szResponse, sizeof(szResponse));
  if (rc) DisplayError(rc);
  rc = DMCWaitForMotionComplete(hdmc, "Z", FALSE);
  if (rc) DisplayError(rc);

  sprintf(szMsg, "PA %ld;BG X", (long)(indent - cnts*mm2i*offset[pos[i]-1]));
  rc = DMCCommand(hdmc, szMsg, szResponse, sizeof(szResponse));
  if (rc) DisplayError(rc);
  rc = DMCWaitForMotionComplete(hdmc, "X", FALSE);
  if (rc) DisplayError(rc);

  fflush(stdin);
  while (kbhit())
```

```
  {
    resp = _getch();
  }
  Sleep(3000);

  rc = DMCCommand(hdmc, "PA 0;BG X", szResponse, sizeof(szResponse));
  if (rc) DisplayError(rc);

  sprintf(szMsg, "Waiting for response...");
  Coord.X = 0;Coord.Y = iRow;iRow ++;
  WriteConsoleOutputCharacter(hConsoleOut, szMsg, strlen(szMsg), Coord, &Dummy);
  while (!_kbhit()) {}
  resp = _getch();
  fprintf(out, "%i %c\n", pos[i], resp);

  rc = DMCWaitForMotionComplete(hdmc, "X", FALSE);
  if (rc) DisplayError(rc);

  sprintf(szMsg, "SP %ld", MaxXSP);
  rc = DMCCommand(hdmc, szMsg, szResponse, sizeof(szResponse));
  if (rc) DisplayError(rc);

  rc = DMCCommand(hdmc, "PA ,0,0;BG Y,Z", szResponse, sizeof(szResponse));
  if (rc) DisplayError(rc);
  rc = DMCWaitForMotionComplete(hdmc, "YZ", FALSE);
  if (rc) DisplayError(rc);
 }
}

long findindent(HANDLEDMC hdmc)
{
 long   i;
 long   rc;
 char   resp;
 char   szMsg[80];
 char   szResponse[32];
 COORD   Coord;
 DWORD   Dummy;

 sprintf(szMsg, "Do you know the appropriate offset? (y or n)");
 Coord.X = 0;Coord.Y = iRow;iRow ++;
 WriteConsoleOutputCharacter(hConsoleOut, szMsg, strlen(szMsg), Coord, &Dummy);
 resp = '\0';
 do
 {
  while (!_kbhit()) {}
  resp = _getch();
 }
 while ((resp != 'n') && (resp != 'y'));

 if (resp == 'y')
 {
  sprintf(szMsg, "Offset = ");
  Coord.X = 0;Coord.Y = iRow;iRow ++;
  WriteConsoleOutputCharacter(hConsoleOut, szMsg, strlen(szMsg), Coord, &Dummy);
  scanf("%ld", &i);
 }
 else
 {
  i = (long)(4*cnts*mm2i);  /* Default to 4 inches */
 }

 sprintf(szMsg, "Going to %ld counts", i);
 Coord.X = 0;Coord.Y = iRow;iRow ++;
 WriteConsoleOutputCharacter(hConsoleOut, szMsg, strlen(szMsg), Coord, &Dummy);
 sprintf(szMsg, "PA %ld;BG X", i);
 rc = DMCCommand(hdmc, szMsg, szResponse, sizeof(szResponse));
 if (rc) DisplayError(rc);
```

```
 rc = DMCWaitForMotionComplete(hdmc, "X", FALSE);
 if (rc) DisplayError(rc);

 resp = '\0';

 ClearScreen(); iRow = 0;
 sprintf(szMsg, "L for +1mm, l for +0.05mm, H for -1mm, h for -0.05mm, q to accept position");
 Coord.X = 0;Coord.Y = iRow;iRow ++;
 WriteConsoleOutputCharacter(hConsoleOut, szMsg, strlen(szMsg), Coord, &Dummy);

 do
 {
  resp = _getch();
  switch(resp)
  {
  case 'L': i += (long)(1*cnts);
     break;
  case 'l': i += (long)(0.05*cnts);
     break;
  case 'H': i -= (long)(1*cnts);
     break;
  case 'h': i -= (long)(0.05*cnts);
     break;
  case 'q': break;
  default:
   sprintf(szMsg, "Invalid Response.  Please type L,l,H,h, or q");
   Coord.X = 0;Coord.Y = iRow;iRow ++;
   WriteConsoleOutputCharacter(hConsoleOut, szMsg, strlen(szMsg), Coord, &Dummy);
  }

  sprintf(szMsg, "PA %ld;BG X", i);
  rc = DMCCommand(hdmc, szMsg, szResponse, sizeof(szResponse));
  if (rc) DisplayError(rc);
  rc = DMCWaitForMotionComplete(hdmc, "X", FALSE);
  if (rc) DisplayError(rc);
 }
 while (resp != 'q');

 ClearScreen(); iRow = 0;
 sprintf(szMsg, "Offset = %ld", i);
 Coord.X = 0;Coord.Y = iRow;iRow ++;
 WriteConsoleOutputCharacter(hConsoleOut, szMsg, strlen(szMsg), Coord, &Dummy);

 sprintf(szMsg, "Hit any key to continue...", i);
 Coord.X = 0;Coord.Y = iRow;iRow += 2;
 WriteConsoleOutputCharacter(hConsoleOut, szMsg, strlen(szMsg), Coord, &Dummy);

 while (!_kbhit()) {};
 resp = _getch();

 rc = DMCCommand(hdmc, "PA 0;BG X", szResponse, sizeof(szResponse));
 if (rc) DisplayError(rc);
 rc = DMCWaitForMotionComplete(hdmc, "X", FALSE);
 if (rc) DisplayError(rc);

 return(i);
}
```

References

[1] D.J. Beebe, C.M. Hymel, K.A. Kaczmarek, M.E. Tyler, "A polyimide-on-silicon electrostatic fingertip tactile display", *IEEE Engineering in Medicine and Biology 17th Annual Conference and 21st Canadian Medical and Biological Engineering Conference*, vol. 2, pp. 1545-6, Montreal, Que., Canada, Sept. 1995.

[2] R.A. Boie, "Capacitive impedance readout tactile image sensor", *IEEE International Conference on Robotics and Automation*, pp. 370-8, Atlanta, GA, USA, 1984.

[3] M. Cohn, M. Lam, and R. Fearing, "Tactile Feedback for Teleoperation", *SPIE Telemanip. Tech.*, vol. 1833, pp. 240-254, 1992.

[4] R.S. Fearing, "Tactile Sensing Mechanisms", *Int. Jnl. of Robotics Research*, vol. 9, no. 3, pp. 3-23, June 1990.

[5] R.S. Fearing, G. Moy, E. Tan, "Some Basic Issues in Teletaction", *IEEE Int. Conf. on Rob. and Auto.*, vol. 4, pp. 3093-9, Albuquerque, NM, USA, April 1997.

[6] H. Fischer, B. Neisius, and R. Trapp, "Tactile Feedback for Endoscopic Surgery", *Interactive Technology and New Paradigm for Healthcare* , ed: K. Morgan, R.M. Satava, H.B. Sieburg, R. Mattheus, J.P. Christensen, pp. 114-117, IOS Press 1995.

[7] R. Ghodssi, D.J. Beebe, V. White, and D.D. Denton, "Development of a Tangential Tactor Using a LIGA/MEMS Linear Microactuator Technology", *1996 Int. Mech. Eng. Cong. and Exposition, Microelectromechanical Systems*, DSC vol. 59, pp. 379-386, Nov. 17-22, 1996.

[8] B. Gray and R.S. Fearing, " A surface-micromachined microtactile sensor array." *IEEE Int. Conf. Rob. and Auto.*, Minneapolis, MN, USA, April 1996.

[9] C.J. Hasser and M.W. Daniels, "Tactile Feedback with Adaptive Controller for a Force-Reflecting Haptic Display", *15th Southern Biomedical Engineering Conf.*, pp. 526-533, Dayton, OH, USA, March 29-31, 1996.

[10] R.D. Howe, "Tactile sensing and control of robotic manipulation", *Advanced Rob.*, vol. 8, no. 3, pp. 245-261, 1994.

[11] R.D. Howe, W.J. Peine, D.A. Kontarinis, and J.S. Son, "Remote Palpation Technology", *IEEE Eng. in Med. and Bio. Mag.*, pp. 318-323, May/June 1995.

[12] R.S. Johansson, U. Landstrom and R. Lundstrom, "Responses of Mechanoreceptive Afferent Units in the Glabrous Skin of the Human Hand to Sinusoidal Displacements", *Brain Research*, vol. 244, pp. 17-25, 1982.

[13] K.A. Kaczmarek, J.G. Webster, P. Bach-y-Rita, and W.J. Tompkins, "Electrotactile and Vibrotactile Displays for Sensory Substitution Systems", *IEEE Trans. on Bio. Eng.*, vol. 38, no. 1, pp. 1-16, January 1991.

[14] K.L. Johnson, *Contact Mechanics*, Cambridge University Press, 1985.

[15] S.J. Lederman, "Heightening tactile impressions of surface texture", *Active Touch*, ed. G. Gordon. Oxford: Pergamon Press, pp. 205-214, 1978.

[16] J.M. Loomis and S.J. Lederman, "Tactual Perception", in *Handbook of Perception and Human Performance*, edited by K.R. Boff, L. Kaufman and J.P. Thomas, pp. 31-1:31-41, John Wiley and Sons: New York, 1986.

[17] M.G. Natrella, *Experimental Statistics*, Department of Commerce, National Bureau of Standards, 1963.

[18] E.J. Nicolson and R.S. Fearing, "The Reliability of Curvature Estimates from Linear Elastic Tactile Sensors", *IEEE Int. Conf. on Rob. and Auto.*, Nagoya, Japan, May 1995.

[19] J.R. Phillips and K.O. Johnson, "Tacile Spatial Resolution II. Neural Representation of Bars, Edges, and Gratings in Monkey Primary Afferents", *J. Neurophysiology*, vol. 46, no. 6, pp. 1192-1203, 1981.

[20] J.R. Phillips and K.O. Johnson, "Tacile Spatial Resolution III. A Continuum Mechanics Model of Skin Predicting Mechanoreceptor Response to Bars, Edges, and Gratings", *J. Neurophysiology*, vol. 46, no. 6, pp. 1204-1225, 1981.

[21] K.B. Shimoga, "Finger Force and Touch Feedback Issues in Dextrous Telemanipulation", *NASA-CIRSSE Int. Conf. on Intel. Rob. Sys. for Space Exploration*, Troy, NY, USA, Sept. 30 - Oct. 1, 1992.

[22] M. Shimojo, M. Shinohara, and Y. Fukui, "Human Shape Recognition Performance for 3D Tactile Display", *IEEE International Conference on Systems, Man, and Cybernetics*, vol. 4, pp. 3192-7, Orlando, FL, USA, Oct. 12-15, 1997.

[23] U. Singh, "Temporal Characteristics of the Human Finger" Master's Report, Dept of EECS, UC Berkeley, May 1997.

[24] M.A. Srinivasan and K. Dandekar, "An Investigation of the Mechanics of Tactile Sense Using Two Dimensional Models of the Primate Fingertip" *J. of Biomechanical Engineering (trans. of the ASME)*, vol. 118, pp. 48-55, 1996.

[25] E. Tan, "Estimating Human Tactile Resolution Limits for Stimulator Design", Master's Report, Dept of EECS, UC Berkeley, May 1995.

[26] Valbo, A.B. and Johanson, R.S. "Detection of Tactile Stimuli. Thresholds of Afferent Units related to pyschophysical thresholds in the human hand", *J. Physiology*, vol. 297, pp. 405-422, 1979.

[27] R. Walpole and R. Myers, *Probability and Statistics for Engineers and Scientists.* Macmillan Publishing Company, 1972.

[28] P.S. Wellman, W.J. Peine, G. Favalora, and R.D. Howe, "Mechanical Design and Control of a High-Bandwidth Shape Memory Alloy Tactile Display", *1997 International Symposium on Experimental Robotics*, Barcelona, Spain, June 1997.